Noname manuscript No.
(will be inserted by the editor)

J. Herault · F. Pétrélis · S. Fauve

1/f noise in turbulent flows

transitions with heavily tailed distributed interevent durations.

Received: date / Accepted: date

Abstract We report the experimental observation of $1/f$ fluctuations in three different turbulent flow configurations: the large scale velocity driven by a two-dimensional turbulent flow, the magnetic field generated by a turbulent swirling flow of liquid sodium and the pressure fluctuations due to vorticity filaments in a swirling flow. For these three systems, $1/f$ noise is shown to result from the dynamics of coherent structures that display transitions between a small number of states. The interevent duration is distributed as a power-law. The exponent of this power-law and the nature of the dynamics (transition between symmetric states or asymmetric ones) select the exponent of the $1/f$ fluctuations.

Keywords 1/f noise · turbulence · rare events

arXiv:1605.09666v1 [physics.flu-dyn] 31 May 2016

1 Introduction

In the past fifty years, a lot of progress has been made in the characterization of coherent structures and their impact on the statistical properties of turbulent velocity fields [1]. Some studies have reported the presence of long range correlations related to $1/f$ noise in the frequency power spectrum of turbulent fluctuations. $1/f$ noise has been observed in the solar wind [2], von Kármán flows [3, 4], magnetohydrodynamic flows [5,6,7,8] and two-dimensional turbulence [8,9]. It has been shown in these studies that $1/f$ noise is related to the slow dynamics of coherent structures but the explicit relation between the spectrum and the dynamics has been emphasized only recently [9]. Originally observed in solid state physics [10], $1/f$ noise (also known as flicker noise) refers to a self-similar power spectrum with an exponent close to -1. This definition has been extended to power spectra of the form $E(f) \propto f^{-\alpha}$, with α between 0 and 2. Such exponents are not unusual in turbulence but the frequency range over which they are observed is. The standard description of turbulent cascade is that velocity fluctuations have energy between the scale of energy injection l_I and the scale of energy dissipation l_d. The corresponding temporal range is limited by τ_I and τ_d, the turn-over time of eddies of size l_I and l_d. However, $1/f$ spectrum in turbulence is observed for frequencies much smaller than τ_d^{-1} and τ_I^{-1}. In other words, no straightforward relation exists between the frequencies and the spatial wave numbers and the usual tools, like the Taylor's hypothesis or dimensional analysis, fail to predict the value of the exponent α. Indeed, we will show that the origin of $1/f$ noise is the dynamics of coherent structures with lifetimes much larger than their turn-over time.

In the context of deterministic dynamical systems, $1/f$ fluctuations were initially discussed by Manneville [11] using a mapping which exhibits long laminar phases interrupted by chaotic bursts. $1/f$ noise is related to a self-similar distribution of waiting times between bursts. More precisely, a signal made of bursts with waiting times τ distributed as τ^{-2}, exhibits a f^{-1} spectrum. In a similar

Helmholtz-Zentrum Dresden-Rossendorf, Bautzner Landstr. 400, 01328 Dresden, Germany · Laboratoire de Physique Statistique, Ecole Normale Supérieure, CNRS, Université P. et M. Curie, Université Paris Diderot, Paris, France

approach, Geisel et al [12] showed that the power spectrum is given by $E(f) \sim f^{-\alpha}$ for a distribution of form $P(\tau) \sim \tau^{\alpha-3}$. Lowen and Teich [13] extended this result to the case of random transitions between symmetric states.

It is tempting to apply the previous approach to coherent structures coexisting with turbulent fluctuations. This requires to identify transitions between different states. It has been shown that two-dimensional turbulence (respectively von Kármán flows) display transitions between symmetric states [14,15] (respectively between different flow patterns [4]). We show here that the statistical properties of these transitions are responsible for the $1/f$ fluctuations. We consider three different quantities: the large scale circulation in two-dimensional turbulence, the magnetic field generated by a von Kármán flow of liquid sodium and the wall pressure fluctuations in a turbulent von Kármán swirling flow. For all these systems, we demonstrate that $1/f$ noise is related to the dynamics of large scale coherent structures that transition between different states. The distribution of the time spent in one of the states follows a power-law with an exponent that sets the value of the exponent of the power spectrum.

The organization of the paper is as follows. In section II the renewal theory and the forecast of Lowen and Teich [13] are recalled. A qualitative argument is presented to understand the connection between the $1/f$ spectrum and self-similar distribution of waiting times. In section III, we analyze the experimental data obtained in the previously mentioned configurations in the light of these theoretical predictions.

2 Renewal process with heavily tailed distributions of interevent durations

2.1 Description

A renewal process is a stochastic process defined by a sequence of N events associated to a series of durations $(\tau_i)_N$, with τ random, positive and independent identically distributed variables. In the following, the events correspond to transitions between two states S called A and B and τ_i is the time spent in one state after the $i-1$ event. We introduce the variable $x(t)$, such that $x(t) = x_A$, when $S = A$ and $x(t) = x_B$, when $S = B$. The distribution of the duration τ is P_A for the state A respectively P_B for B. A process is symmetric when $P_A = P_B$. Figure 1 (top) illustrates a symmetric renewal process with $x_A = 1$ and $x_B = -1$.

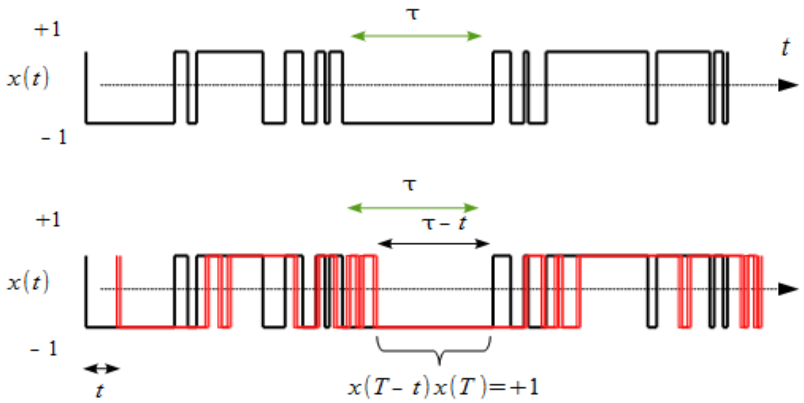

Fig. 1 Top: renewal process defined by random transitions between two-states, associated to the values $x = \pm 1$. Bottom : the auto-correlation function $C(t)$ is given by the integration of the product $x(T)x(T-t)$, which is mostly made of long phases of constant polarity and phases of fast oscillations. The former phases contribute to the long-range correlation.

The power spectrum of x is defined by

$$E(f) = \frac{1}{T_f} \langle \hat{x}(f)\hat{x}^*(f) \rangle \quad \text{with} \quad \hat{x}(f) = \int_0^{T_f} x(t) e^{i2\pi f t} dt \tag{1}$$

where $\langle \cdot \rangle$ is the average over the realizations and $T_f = \sum_{i=1}^{N} \tau_i$ is the duration of the process, that ultimately tends to infinity. In this study, we are interested in self-similar power spectrum with $E(f) \sim f^{-\alpha}$, and $0 < \alpha < 2$.

2.2 Relation between the exponents α and β

We start with a qualitative argument to explain how the distribution $P(\tau) \sim \tau^{-\beta}$ controls the value of the exponent α [13]. To wit, we first obtain the auto-correlation $C(t)$ of x and then we calculate the power-spectrum of x using the Wiener-Khinchin theorem. The autocorrelation function $C(t)$ is defined by

$$C(t) = \langle x(0)x(t) \rangle \tag{2}$$

The Wiener-Khinchin theorem states that the Fourier transform of $C(t)$ converges to $E(f)$ for $T_f \to \infty$. We consider a symmetric process with $x_A = 1$ and $x_B = -1$ as sketched in figure 1 (bottom). We fix $\beta > 2$, in order to consider only processes with $\langle \tau \rangle < \infty$. For an ergodic process and $T_f \gg \langle \tau \rangle$, the auto-correlation $C(t)$ is obtained by

$$C(t) = \frac{1}{T_f} \int_0^{T_f} x(T-t)x(T) dT \tag{3}$$

We observe that the product $x(T)x(T-t)$ is composed of fast oscillations and long periods of constant polarity, due to long phases of duration τ in $x(T)$. We assume that only the phases with $\tau > t$ contribute to the autocorrelation with a contribution $\tau - t$. In other words, the average contributions of short phases with $\tau < t$ vanish. It follows that the autocorrelation is well approximated by

$$C(t) \simeq \frac{1}{T_f} \int_t^{T_f} (\tau - t) n(\tau) d\tau \quad \text{for} \quad \langle \tau \rangle \ll t \ll T_f \tag{4}$$

with $n(\tau)$ the number of phases of duration τ, which is equal to $P(\tau)T_f/\langle \tau \rangle$, with $T_f/\langle \tau \rangle$ the total number of events. Then, equation (4) becomes

$$C(t) \simeq \frac{1}{\langle \tau \rangle} \int_t^{T_f} (\tau - t) P(\tau) d\tau. \tag{5}$$

If $P(\tau)$ is an exponential function, the autocorrelation function is also an exponential function, as expected for a Poisson process. For $P(\tau) \sim \tau^{-\beta}$ and $\beta > 2$, the autocorrelation scales as $C(t) \sim t^{-\beta+2}$. Finally, the power spectrum $E(f)$ is given by the Fourier transform of $C(t)$

$$E(f) \sim f^{\beta-3} \int u^{-\beta+2} e^{-2\pi u i} du \tag{6}$$

with the change of variable $u = ft$ and for $T_f \to \infty$. We thus obtain $\alpha = 3 - \beta$. The result is extended to $1 < \beta < 2$ [13,16] by considering a distribution with $P \sim \tau^{-\beta}$ for $\tau_i \ll \tau \ll \tau_e$, and zero otherwise or exponentially distributed. For a symmetric process ($P_A = P_B$), the power spectrum is then given by

$$E(f) \sim \begin{cases} f^{-(3-\beta)} & \text{for} \quad 1 < \beta < 3 \\ \ln(\tau_i f) & \text{for} \quad \beta = 3 \end{cases} \tag{7}$$

for $\tau_e^{-1} \ll f \ll \tau_i^{-1}$.

Bursting processes have been considered. The signal $x(t)$ is composed of short intermittent bursts separated by intervals τ distributed as $P \sim \tau^{-\beta}$ (see figure 2). The result differs from the symmetric

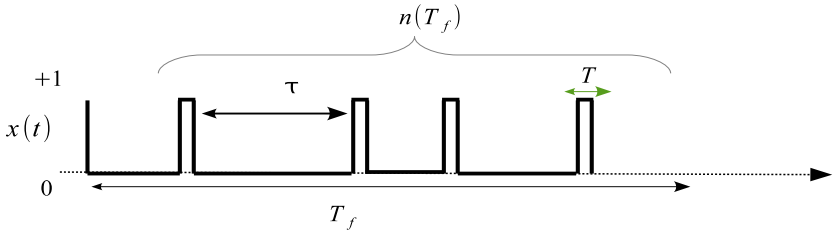

Fig. 2 Time series displaying bursts from $x = 0$ to $x = 1$. The process is asymmetric and the duration of the low amplitude phases is distributed according to a power-law, $P \sim \tau^{-\beta}$. In contrast the large amplitude phases have durations that are not distributed following a heavy tailed distribution.

case when $\beta < 2$. Consider a time series for which $x(0) = 1$. Let $n(T_f)$ be the number of bursts within a time interval of length T_f. We estimate

$$S = \int_0^{T_f} x(0)x(t)dt \simeq n(T_f)T \tag{8}$$

where T is the duration of a bursts. The number of burst is roughly, $n(T_f) = T_f/\langle\tau\rangle_{T_f}$ where $\langle\tau\rangle_{T_f}$ is the average duration of the $x = 0$ phases when we consider a time series of duration T_f. For $\beta < 2$, $\langle\tau\rangle_{T_f}$ does not tend to a constant at large T_f, which obviously results from the divergence of the first moment of the distribution P. Then an estimate of $\langle\tau\rangle_{T_f}$ is given by

$$\langle\tau\rangle_{T_f} = \int_0^{T_f} \tau P(\tau)d\tau \simeq T_f^{2-\beta} \tag{9}$$

We thus have $n(T_f) \simeq T_f^{\beta-1}$. Averaging S over realizations and differentiating with respect to T_f, we obtain the autocorrelation function as $C(t) \propto t^{\beta-2}$. The exponent of the power spectrum then satisfies $\alpha = \beta - 1$.

To sum up, the predictions for the power spectrum of a bursting process are [13,16]

$$E(f) \sim \begin{cases} f^{-(\beta-1)} & \text{for} \quad 1 < \beta < 2 \\ \ln(f\tau_i)^{-2} f^{-1} & \text{for} \quad \beta = 2 \\ f^{-(3-\beta)} & \text{for} \quad 2 < \beta < 3 \\ \ln(\tau_i f) & \text{for} \quad \beta = 3 \end{cases} \tag{10}$$

We note that for symmetric or bursting processes, α is equal to $3 - \beta$ for $\beta > 2$. It implies that the effect of asymmetry in the process is relevant only for distributions with $\beta < 2$.

These results hold for a range of frequencies f corresponding to the inverse range of durations τ. In particular, if $P(\tau)$ displays a cut-off for time larger than τ_e, $1/f$ noise may be observed down to the low cutoff frequency τ_e^{-1}. This property allows us to consider $1/f$ noise with low frequency cut-off τ_e^{-1}, related to an exponential decay of $P(\tau)$ for $\tau \gg \tau_e$.

3 Application to turbulent time series

We now illustrate how coherent structures generate a $1/f$ spectrum in three different configurations involving turbulent flows. After shortly describing the experiments, we identify transitions in the time series. We then show that the measured exponents α of the power-spectrum and β of the distribution of waiting times follow the theoretical predictions of section 2, which depend on the value of β and on the nature of the process (bursting or symmetric). We recapitulate the results in the following table.

System	Variable	Process	α	β	Relation
Two-dimensional turbulence	flow rate	symmetric	0.7	2.25	$\alpha = 3 - \beta$
Von Kármán Sodium Dynamo	magnetic field	bursting	0.5	2.5	$\alpha = 3 - \beta$
Von Kármán flow	pressure	bursting	0.6	1.58	$\alpha = \beta - 1$

Table 1 Summary of the experimental results. We recall the experimental configuration (first column), the measured variable (second column), the nature of the process (third column), the measured exponents α and β and the expected relation between them, depending on the value of β and on the nature of the process.

3.1 Two-dimensional turbulence

The experiment consists in driving a flow with an electromagnetic force in a conducting fluid, as described in Refs. [14]. A thin layer of liquid metal (Galinstan) of thickness $h = 2cm$, is contained in a square cell of length L= 12 cm. The cell is located inside a coil producing a uniform vertical magnetic field of strength $B_0 = 0.98$T. A DC current I (0-200A) is driven through the bottom of the cell using a periodic array of 8 electrodes with alternate polarities. The density current $\mathbf{j}$ is radial close to each electrode. The Lorentz force $\mathbf{f}_L = \mathbf{j} \times \mathbf{B}_0/\rho$, with ρ the density, creates locally a torque. For small injected currents, the laminar flow corresponds to an array of 8 counter-rotating vortices shown in figure 3 (top, center). The flow remains mostly two-dimensional, due to Ohmic dissipation of the perturbations with velocity dependence along the direction of the magnetic field.

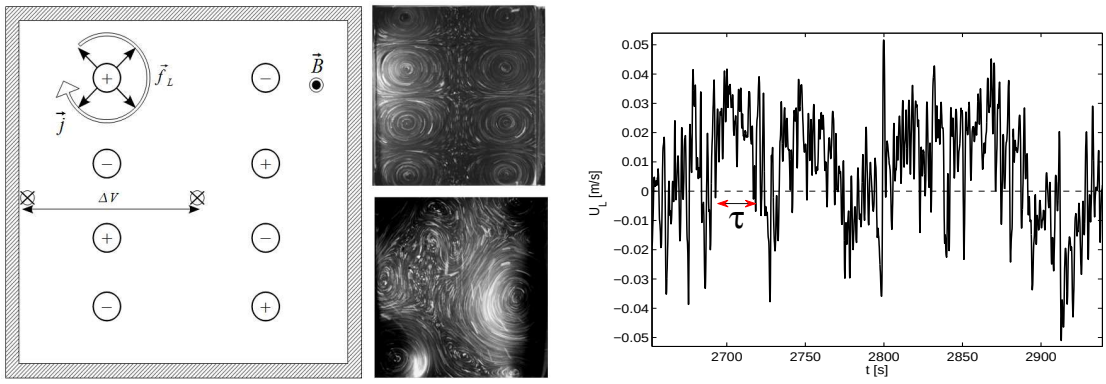

Fig. 3 Left: Schematics of the experimental set-up. The Lorentz-force close to the electrodes generates an array of height counter-rotating vortices in the laminar regime (center top picture). The turbulent flow (center bottom picture) is characterized by coherent vortices forcing a large scale circulation. The flow rate is measured between the center and the wall, using the induced voltage ΔV. Right: time series $U_L(t)$ of the flow rate divided by the distance $L/2$ for $Rh = 15$.

When the forcing is strong enough, the flow becomes turbulent (Fig.3, left). Two-dimensional turbulence is characterized by an inverse cascade of energy. The energy is transferred to large scales and coherent structures display lifetimes larger than their turn-over time. The dissipation is mostly provided by the friction of the bulk flow with the bottom boundary layer for very large Reynolds number Re. The ratio between the forcing and the dissipation that results from bottom friction is given by the dimensionless number Rh. Typically, the flow becomes turbulent for $Rh \simeq 5$ and coherent structures appear for $Rh \simeq 12$.

The velocity measurements are performed with a pair of electric potential probes (Fig. 3): one is located in the middle of the cell and the other one close to the lateral wall. The probes measure a potential difference ΔV, due to the integral contribution of the local electromotive force $E = -\mathbf{u} \times \mathbf{B}_0$. Thus, $\Delta V = \phi_L B_0$, with ϕ_L the flow rate between the center and the wall of the cell. We use the velocity amplitude U_L, defined by $U_L = \phi_L/(L/2)$. Due to flow rate conservation, the velocity amplitude U_L is

also equal to the averaged azimuthal velocity. The voltage is sampled at a frequency rate $f_r = 10$Hz. A typical time series $U_L(t)$ is shown in fig. 3 (right).

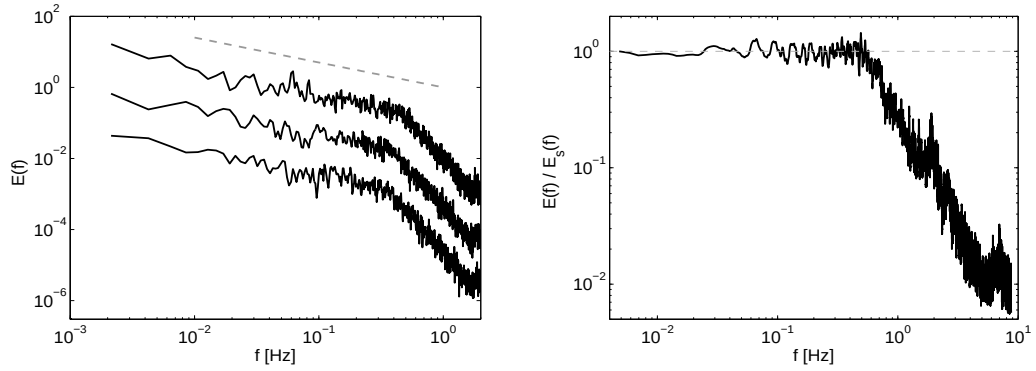

Fig. 4 Left: frequency power spectra $E(f)$ of $U_L(t)$ for $Rh = 16, 19, 24$ (from bottom to top). For clarity, the spectra have been multiplied by 1, 10 and 100. The $f^{-0.7}$ law is displayed as a dashed line. Right: ratio of the power spectra of $s(t)$ and $U_L(t)$, rescaled such that it tends to 1 for $f \to 0$.

These time series exhibit $1/f$ power spectrum over one decade (Fig. 4) for $2.10^{-2} < f < 2.10^{-1} Hz$. The related frequencies are smaller than τ_D^{-1} the damping rate of the friction and smaller than the inverse of the turn-over time $\tau_L = L/\sigma_U$, with σ_U the standard deviation of U_L. In the context of 2D turbulence, τ_L^{-1} corresponds to the smallest frequency of the turbulent cascade. Thus the observed $1/f$ spectrum is not directly related to the energy cascade, but to the coherent dynamics of the large scale circulation. A systematic study of the exponents α, defined by $E(f) \sim f^{-\alpha}$, shows that their value is almost constant and equal to 0.7 for $Rh \in [15, 28]$ (black circles, Fig. 5).

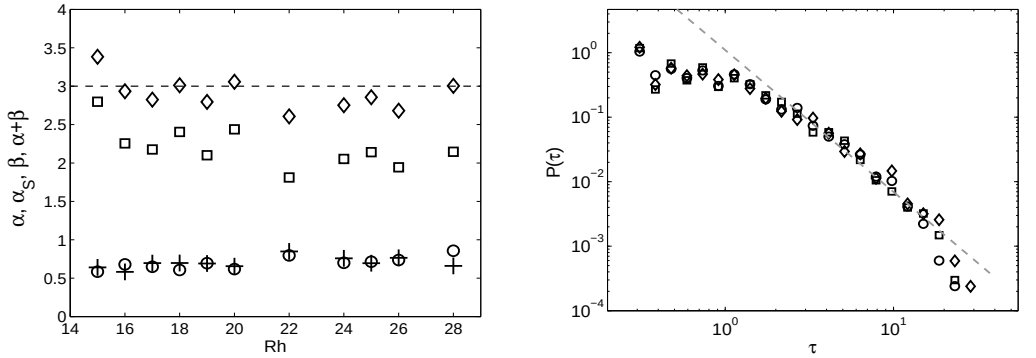

Fig. 5 Left : Exponents α (circle) and β (square) for times series with different Rh. The exponent of the spectrum of $x(t)$ (plus) and the sum $\alpha + \beta$ are (diamond) also illustrated. Right : distribution $P(\tau)$ of the waiting time τ between sign change for $Rh = 16, 19, 24$. The dashed line follows the law $\tau^{-2.25}$.

A closer inspection shows that the time series U_L is composed of long phases of constant polarity of duration τ superimposed with random fluctuations. In Fig. 3, we highlight a phase of constant polarity with duration τ of 20 s (see the event indicated by a double-arrow). The inverse of this time τ^{-1} matches with the range of frequency of the $1/f$ spectrum. Due to the symmetry of the forcing, U_L displays random transitions between both polarities. In order to show that these transitions generate the $1/f$ noise, we decompose the signal U_L into a two-state signal $s(t)$, which is defined by the sign

of U_L, *i.e.* $s \equiv \text{sign}\,(U_L)$. A typical time series s is composed of one thousand transitions from one direction of rotation to the other. The ratio of the power spectrum of U_L and of s is reported in fig. 4 and is almost constant over the frequency range corresponding to the $1/f$ spectrum. Thus both power spectra have the same behaviour at low frequency. A systematic study of the exponent α_s of the power spectrum of $s(t)$ (black cross in fig. 5) shows that its value is very close to the exponent α (black circles). This implies that the slow dynamics of U_L, which is responsible for the $1/f$ noise, is mostly contained in $s(t)$.

We calculate the probability density function of the duration between sign changes of s and report it in Fig. 5 (right). The distributions exhibit a power-law behavior on a range of durations $\tau \in [2, 40]s$ corresponding to the inverse of the range of frequencies $f \in [2.10^{-2}, 2.10^{-1}]$ Hz of the $1/f$ noise. We recover the association of a self-similar distribution of interevent duration with a self-similar spectrum of the time series. A systematic measurement of the exponent β (black square, fig. 5), defined by $P(\tau) \sim \tau^{-\beta}$, shows that it fluctuates around the value $\beta = 2.25$.

The sum $\alpha + \beta$ (diamonds in fig. 5) remains close to 3, as predicted by equation (7) for a symmetric renewal process. All the previous results converge to the conclusion that the random changes of the sign of U_L with waiting time distributed as $P \sim \tau^{-2.25}$, is at the origin of the observed $1/f$ noise.

3.2 Dynamics of the magnetic field generated by a von Kármán flow of liquid sodium

The generation of magnetic field by a turbulent flow of liquid sodium has been widely studied in the VKS experiment, described in detail in ref. [7]. The flow is driven by two counter-rotating coaxial impellers in a cylindrical vessel (see fig. 8). When the rotation rate of the impellers is larger than a critical frequency F_c, a magnetic field is generated by a self-sustained induction process, called the dynamo instability. The large scale magnetic field is mostly a stationary axial dipole with superimposed magnetic fluctuations due to the strong turbulence of the flow. $1/f$ noise in the power spectrum of the magnetic field has been reported in dynamo regimes [7] and also below the dynamo threshold when an external magnetic field is imposed to the turbulent flow of liquid sodium [5]. We consider below the dynamo case but the same analysis hold for both.

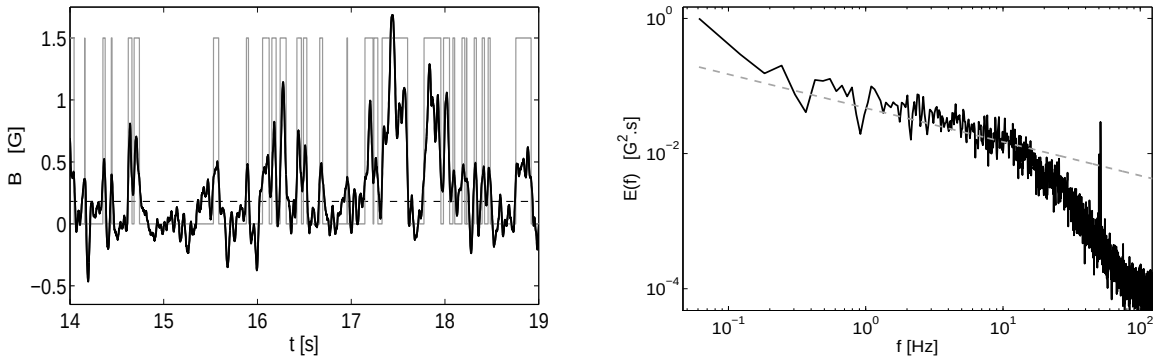

Fig. 6 Left: time series $B(t)$ of the azimuthal magnetic field, fluctuating around its mean value (dashed line). The grey line corresponds to the bursting process $s(t)$ extracted from $B(t)$. Right: power spectrum of $B(t)$ displaying a $f^{-0.5}$ behavior at low frequency (dashed line).

Measurements of the azimuthal magnetic field $B(t)$ are performed inside the vessel in the mid-plane between the impellers for $F = 20$ Hz (just above the dynamo threshold). The measurements of other components of magnetic field show similar results. A time series of $B(t)$ is displayed in fig. 6 together with the power spectrum which exhibits a clear $f^{-\alpha}$ spectrum with $\alpha \simeq 0.5$ for $f \in [1.5, 15]Hz$. For $f > 20$ Hz, the power-spectrum scales as $f^{-11/3}$, due to the passive streching of the magnetic field by the small scale turbulent fluctuations.

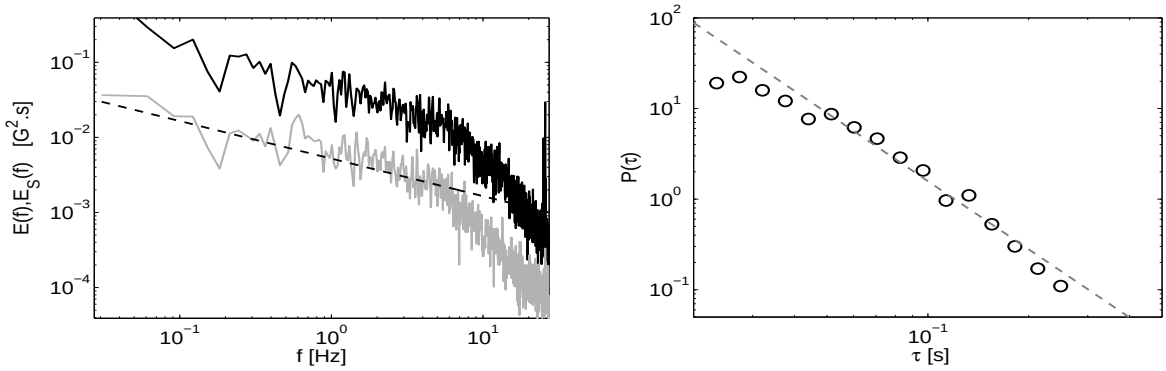

Fig. 7 Left : power spectrum of $B(t)$ (black line) and $s(t)$ (grey line) compared to the law $f^{-0.6}$ (dashed line). Right : distribution of the waiting time τ between bursts, with the law $\tau^{-2.5}$ (dashed line).

As observed in fig. 6, the magnetic field $B(t)$ displays bursts with amplitudes up to 8 times the average value. We thus define a two-states signal $s(t)$ given by phases of weak and large amplitude. Among the possible criteria to define a burst, we consider a threshold larger than the average value of B, such that above (resp. below) it, the system is in the high (resp. low) amplitude state. The resulting two-states signal $s(t)$ is displayed in fig 6 (left) in grey. The power-spectrum of $s(t)$ (in grey) is compared to the one of B (in black) in fig. 7 (left). At low frequency, both power spectra follow the same power-law. The distribution $P(\tau)$ of waiting times τ between bursts is displayed in fig. 7 (right). For the range of duration $\tau \in [5.10^{-2}, 25.10^{-2}]s$, $P(\tau)$ follows a power-law $\tau^{-\beta}$ with $\beta \simeq 2.5$.

We know from equation (10) holding for burst processes, that α should be equal to $3 - \beta$. The bursting process observed in the VKS experiment follows this relation with $\alpha = 0.5$ and $\beta = 2.5$.

3.3 Pressure fluctuations in von Kármán swirling flows

$1/f$ noise has been also reported for the pressure signal in von Kármán swirling turbulent flows in water [3]. The results presented below are extracted from this reference where a detailed description of the experiment can be found. The pressure $p(t)$ is measured on the lateral boundary of the cylinder. Pressure drops are observed that are due to vorticity concentrations passing close to the pressure probe.

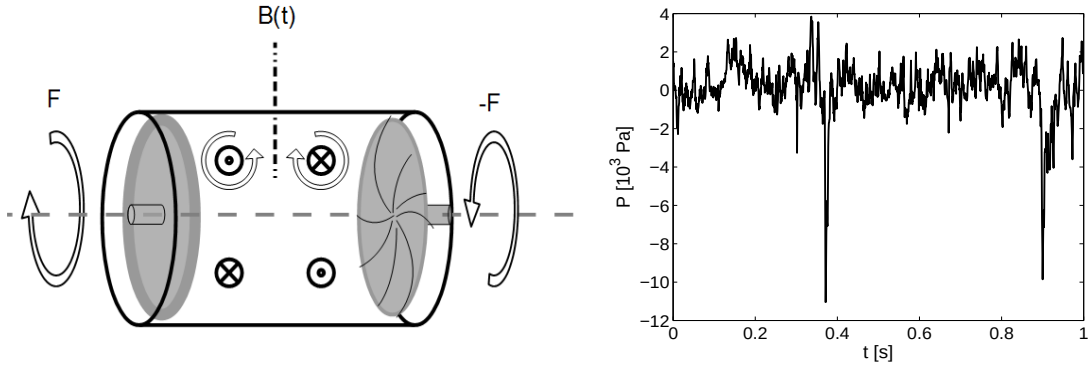

Fig. 8 Left : Sketch of the VKS and von Kármán experiments : two impellers counter-rotate at frequency F. The vertical thick line indicates the location of the magnetic probes in the VKS experiment. Right : time series $p(t)$ of the wall pressure from Abry et al. [3].

The time series of $p(t)$ displaying large pressure drops is shown in fig. 8 (right). The related power-spectrum is shown in fig. 9 (left, black circles) and exhibits $1/f$ noise at low-frequency with an exponent $\alpha = 0.6$. It has been shown in ref. [3] that removing the pressure drops from the signal using a wavelet technique, almost suppresses the $1/f$ noise from the power-spectrum of the filtered signal $\tilde{p}$ (fig. 8, left, black diamonds). We observe again in this example that the $1/f$ noise results from the bursts. Thus, we define a two-state signal that consists of the long phases of weak amplitude between successive bursts and the short phases of large amplitude pressure drops (the bursts). The distribution of waiting times between successive bursts is displayed in fig. 9 (right) and exhibits a power-law in the range $\log(\tau) \in [-1.7, -0.5]$ (*i.e.* $\tau \in [0.02, 0.3]$ s) corresponding to the frequency range $\log(f) \in [0.6, 1.8]$ (*i.e.* $f \in [4, 60]$ Hz) of the $1/f$ noise. In this range, the fitted exponent is $\beta = 1.58$. We also remark that the distribution has an exponential tail, but only for durations larger than the inverse of the minimum frequency over which $1/f$ noise is observed.

In contrast to the previous case, the exponent β is smaller than 2 and the theoretical prediction is then $\alpha = \beta - 1$. Once again, the agreement between the prediction and the fitted exponents is very good with $\beta - 1 = 0.58$ and $\alpha = 0.6$.

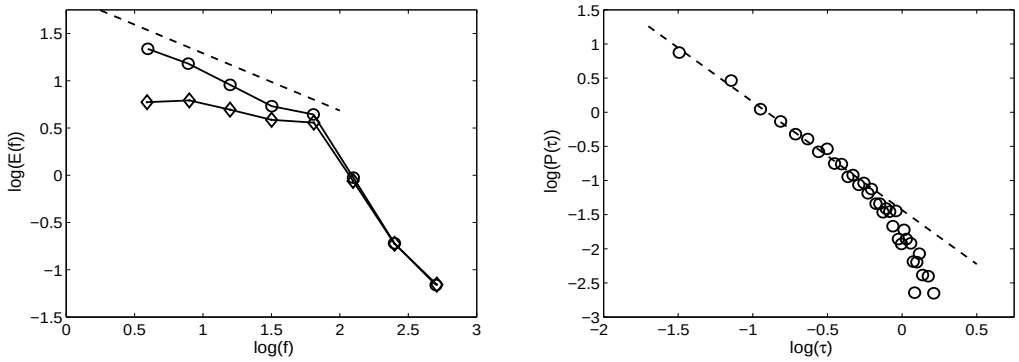

Fig. 9 Left : power spectra of $p(t)$ (circle) and $\tilde{p}$ (diamonds), the filtered pressure without bursts. The dashed line indicates the law $f^{-0.6}$. Right : distribution of the waiting time between pressure drops. The law $\tau^{-1.58}$ is displayed with a dashed line.

4 Conclusion

We have shown that the $1/f$ fluctuations observed experimentally in three different turbulent flows are related to the coherent dynamics of large scale structures, which randomly transition between different states. The dynamics is characterized by the nature of the process (asymmetric bursts or symmetric transitions), and by the power-law distribution of the interevent durations. These two properties fully determine the exponent of the power spectrum.

Acknowledgements The authors acknowledge their colleagues of the VKS team with whom the experimental data have been obtained.

References

1. Hussain, A. K. M. : J. Fluid Mech. **173**, 303-356 (1986)
2. Matthaeus, W. H., Goldstein M. L. : Phys. Rev. Lett. **57**, (1986)
3. Abry, P., et al: J. Phys. II **4**, 725-733 (1994)
4. Ravelet, F. , Chiffaudel, A., Daviaud, A.: J. Fluid Mech. **601**, 339-364 (2008)
5. Bourgoin, M. et al.: Phys. Fluids **14**, 3046 (2002)
6. Ponty, Y., Politano, H., Pinton, J. F. : Phys. Rev. Lett. **92**, 144503 (2004)

7. Monchaux, R., et al.: Phys. Fluids **21**, 035108 (2009)
8. Dmitruk, P., et al.: Phys. Rev. E **83**, 066318 (2011)
9. Herault, J. : PhD Thesis : *Dynamique des structures coherentes en turbulence magnetohydrodynamique*, Paris 7, (2013)
10. Van Der Ziel, A. : Physica D **16**, 359-372 (1950)
11. Manneville, P.: J. Physique **41**, 1235-1243 (1980)
12. Geisel, T., Zacherl,A., Radons, G. : Phys. Rev. Lett. **59**, 2503 (1987).
13. Lowen, S.B., Teich M.C. : Phys. Rev. E **47**, 992 (1993)
14. Sommeria, J. : J. of Fluid Mech. **170**, 139-168 (1986)
15. Gallet, B. et al. :Geophys. Astrophys. Fluid Dyn. **106**, 468-492 (2012)
16. Niemann, M., Kantz, H., Barkai, E. : Phys. Rev. Lett. **110**, 140603 (2013)